



THE UNIVERSITY *of* EDINBURGH

## Edinburgh Research Explorer

### **Epoxy based hybrid nanocomposites: Fracture mechanisms, tensile properties and electrical properties**

**Citation for published version:**

Bajpai, A, Martin, R, Ibarboure, E & Faria, H 2021, 'Epoxy based hybrid nanocomposites: Fracture mechanisms, tensile properties and electrical properties', *Materials Today: Proceedings*, vol. 34, no. 1, pp. 210-216. <https://doi.org/10.1016/j.matpr.2020.02.797>

**Digital Object Identifier (DOI):**

[10.1016/j.matpr.2020.02.797](https://doi.org/10.1016/j.matpr.2020.02.797)

**Link:**

[Link to publication record in Edinburgh Research Explorer](#)

**Document Version:**

Publisher's PDF, also known as Version of record

**Published In:**

Materials Today: Proceedings

**General rights**

Copyright for the publications made accessible via the Edinburgh Research Explorer is retained by the author(s) and / or other copyright owners and it is a condition of accessing these publications that users recognise and abide by the legal requirements associated with these rights.

**Take down policy**

The University of Edinburgh has made every reasonable effort to ensure that Edinburgh Research Explorer content complies with UK legislation. If you believe that the public display of this file breaches copyright please contact [openaccess@ed.ac.uk](mailto:openaccess@ed.ac.uk) providing details, and we will remove access to the work immediately and investigate your claim.





Contents lists available at ScienceDirect

## Materials Today: Proceedings

journal homepage: [www.elsevier.com/locate/matpr](http://www.elsevier.com/locate/matpr)

## Epoxy based hybrid nanocomposites: Fracture mechanisms, tensile properties and electrical properties

A. Bajpai<sup>a,\*</sup>, R. Martin<sup>b</sup>, H. Faria<sup>c</sup>, E. Ibarboure<sup>a</sup>, S. Carlotti<sup>a</sup><sup>a</sup> Univ. of Bordeaux, CNRS, Bordeaux INP, LCPO, UMR 5629, F-33600 Pessac, France<sup>b</sup> Department of Mechanical Engineering, University of Salamanca, Higher Polytechnic School of Zamora, Campus Viriato, Spain<sup>c</sup> University of Aveiro, Portugal

## ARTICLE INFO

## Article history:

Received 1 September 2019

Received in revised form 18 February 2020

Accepted 24 February 2020

Available online xxxx

## Keywords:

Epoxy

Nanocomposite

Fracture mechanics

Nanoparticles

Electrical properties

## ABSTRACT

This work explore the effect of addition of a combination of rigid nanofillers and core-shell rubber nanoparticles on the fracture mechanics, tensile, electrical and thermo-mechanical properties of epoxy resins. SiO<sub>2</sub> nanoparticles, multi-walled carbon nanotubes (MWCNT's), as rigid nanofillers, and core-shell rubber (CSR) nanoparticles, as soft nanofillers were used with bisphenol-A based epoxy resin. Further, the rigid fillers were added systematically with core-shell rubber nanoparticles and MWCNT's to study the combined effect of rigid nanofillers and soft CSR nanoparticles. The resulting systems will be characterized by standard methods. This includes a thorough characterization of tensile, fracture mechanics, electrical, and thermal properties. The results show that the maximum increase of fracture toughness (207%) and fracture energy (910%) was obtained for system containing 5 wt% of CSR and 10% SiO<sub>2</sub>. The electrical conductivity threshold was obtained at 0.075 wt% of MWCNT's modified system. The introduction of CSR nanoparticles significantly increase the fracture energy of the matrix with decrease in tensile strength and tensile modulus, which was further recovered with the addition of SiO<sub>2</sub> nanoparticles. The analysis of the fracture surfaces revealed the toughening micro-mechanisms.

© 2020 Elsevier Ltd. All rights reserved.

Selection and peer-review under responsibility of the scientific committee of the 12th International Conference on Composite Science and Technology. This is an open access article under the CC BY-NC-ND license (<http://creativecommons.org/licenses/by-nc-nd/4.0/>).

## 1. Introduction

Epoxy resins belong to a class of highly cross-linked thermoset polymers used most often with reinforcing fibers in a wide range of composite applications, e.g. automotive, aerospace, and pressure vessels [1]. They show a high specific strength, high modulus, dimensional stability, and low creep [2]. The high cross-link density makes them inherently brittle materials as they were unable to resist crack initiation and propagation effectively, i.e. epoxies have a low fracture toughness. The fracture energy can be increased by adding dispersed rubber to the epoxy resin [3]. Nevertheless, these materials were unfavourable to strength and thermo-mechanical properties of epoxy, especially, the glass transition temperature  $T_g$  [4]. Another route of increase the fracture toughness of epoxy polymers is to use core shell rubber (CSR) nanoparticles. They consist of a rubbery core and a resin suited shell material, which is only a few nanometers thick. These mod-

ifiers incorporate the toughening mechanisms of rubber based modifiers, e.g. cavitation, plastic void growth and subsequent shear yielding [5] together with a good adherence to the matrix, due to a modified shell material [6,7]. The addition of rigid fillers like MWCNT's [8], TiO<sub>2</sub> [9], Al<sub>2</sub>O<sub>3</sub> [10], Glass [11], and SiO<sub>2</sub> [12–14] can improve the strength and modulus of epoxy nanocomposites while also increasing the fracture toughness without decreasing the glass transition temperature of the nanocomposites. Though the rubber toughened epoxy system gained importance for the improvement of the impact properties of cured epoxy, there was a significant decrease in the modulus and thermal stability of the materials. So, the search for alternative toughening method led to discover a new method using two different types of fillers simultaneously. While one will increase the fracture toughness, the other may increase at the same time the modulus and glass transition temperature. Such a type of approach is known as hybrid toughening, and this was first adapted by Kinloch et al. [15] who tried to restore the lost stiffness caused by the application of rubber modification. Since then, several researchers have started examining many combinations of different sized particles for

\* Corresponding author.

E-mail address: [ankur0062001@gmail.com](mailto:ankur0062001@gmail.com) (A. Bajpai).<https://doi.org/10.1016/j.matpr.2020.02.797>

2214-7853/© 2020 Elsevier Ltd. All rights reserved.

Selection and peer-review under responsibility of the scientific committee of the 12th International Conference on Composite Science and Technology.

This is an open access article under the CC BY-NC-ND license (<http://creativecommons.org/licenses/by-nc-nd/4.0/>).

hybrid toughening. The following systems were examined by different researchers, e.g. SiO<sub>2</sub> and CSR [16,17], BCP and TiO<sub>2</sub> nanoparticles [9], and CTBN-rubber and CNT [18,19]. However, no synergies were observed in the case of BCP-CNT hybrids [8]. Recently some researchers reported hybrid toughening of block co-polymers and CSR nanoparticles [7,20].

Polymeric materials have high resistivity and come into the category of insulators. Various fillers can be introduced in polymers to reduce their resistivity and can be used for various applications as their resistivity decreases with respect to the filler. The intrinsic conductivity of fillers, their aspect ratio, interactions between polymer and filler surface, their distribution and orientation were critical parameters to obtain the conductivity and their percolation threshold [21,22]. The CNT based polymer nanocomposite attracted researchers because of their superior mechanical and electrical properties. Previous studies revealed that addition of small amount of CNT's (<1 wt%) to epoxy matrix can increase the electrical, mechanical and thermal properties with affecting the processability of composites [23].

It can be inferred that much work was reported for fracture mechanics and toughening mechanisms of different type of modifiers with a bisphenol A based epoxy system. However, limited work was reported for the effect of different modifiers on the tensile properties of low viscosity epoxy/hardener system which was further to be used in filament winding process for the production of different type of composite based pressure vessels. The purpose of this paper was to show the effect of SiO<sub>2</sub>, multi walled carbon nanotubes (MWCNT's) and core shell rubber (CSR) nanoparticles loading on the mechanical, electrical, and thermal properties of a low viscosity epoxy resin and anhydride based hardener system. The differential scanning calorimetry (DSC) and dynamic mechanical analysis (DMA) were performed to evaluate thermal performance. The tensile tests and fracture test were performed to evaluate mechanical performances. Four point probe method was used to evaluate the conductivity of tailored nanocomposites. Microscopic techniques were used to investigate the dispersion of CNT's, SiO<sub>2</sub> nanoparticles, CSR and material's failure mechanisms. The obtained results were to be used as the matrices for the development of innovative low-, mid- and high-pressure tanks based on advanced composite materials and processes.

## 2. Materials

The CA144 (diglycidyl ether of bisphenol A) liquid epoxy resin produced by Sika Axson, manufactured from epichlorohydrin and bisphenol-A which has an epoxy equivalent weight (EEW) of 187 g.eq<sup>-1</sup>. The CH141 anhydride based curing agent and accelerator CR144 were supplied by Sika Axson. The resin, hardener and accelerator were used in the ratio of 100: 90: (1–4). The mixed viscosity of the system was 800 mPa.s [24] at 25 °C. The MWCNT's (20 nm) were supplied by Nanocyl, Belgium in the form of 2 wt%

**Table 2**

Conductivity of different modified epoxy nanocomposites.

Samples	Conductivity (S/m)
EP_Ref	–
EP_0.05 CNT	–
EP_0.075CNT	0.00026 (±0.00005)
EP_0.1CNT	0.00163 (±0.00002)
EP_0.075 CNT_10 SiO <sub>2</sub>	0.00022 (±0.00003)
EP_0.075 CNT_5 CSR	0.00021 (±0.00006)

masterbatch in bisphenol A based epoxy resin. The CSR nanoparticles (dia. 200 nm) used in this work were Kane Ace MX267 supplied by Kaneka Belgium NV which has epoxy equivalent weight of 269 g.eq<sup>-1</sup>. The material supplied was in the form of a masterbatch which was a 37 wt% concentrate of core-shell rubber toughening agent in unmodified liquid epoxy resin based on bisphenol-F based epoxy system [25]. The SiO<sub>2</sub> nanoparticles (dia. 20 nm) Nanopox F520 supplied by evonik industries in the form of master batch which contains 40 wt% of SiO<sub>2</sub> nanoparticles dispersed in bisphenol-F based epoxy system. The respective amount of modifier was added to the resin and mixed with a dissolver aggregate, then heated up to 100 °C until a homogenous solution was reached and optical transparency observed (for SiO<sub>2</sub> nanoparticles and CSR modified systems). For curing masterbatch of SiO<sub>2</sub>/ CSR/ MWCNT's were diluted with neat resin at 50 °C to the targeted concentration, and then a stoichiometric amount of curing agent was added. This mixture was stirred for 20 min. at 100 °C. Finally, the reactive system was casted into PTFE molds, which were coated with a PAT-607/FB (E. und P. Würtz GmbH & Co KG, Germany) release agent. The samples were cured using a three step curing cycle: (1) 80 °C for 3 h, (2) 120 °C for 3 h, and (3) 140 °C for 3 h. Different systems prepared in this study were shown in Table 1.

## 3. Experimental methods

### 3.1. Differential scanning calorimetry

The DSC experiments were performed on a Q100 (TA instruments) system to determine exotherm and glass transition temperature (T<sub>g</sub>). Firstly, fresh prepared epoxy/hardener system with modifier was weighed (~3–5 mg) and placed in a crucible, sealed with lids with the help of crucible sealing press. In the first cycle, the sample was heated from room temperature up to 200 °C, cooled down to room temperature, and again heated to 200 °C with a heating rate of 10 °C/min.

### 3.2. Dynamic-mechanical thermal analysis

In the present study, the storage modulus, the loss modulus, and tan δ of all the bulk samples were measured by dynamic mechanical thermal analysis using a DMA RSA3 machine from TA

**Table 1**

Composition and nomenclature of bulk epoxy based composites. In notation (EP\_x Y) EP denotes the reference epoxy / hardener system and x represents the wt% used, and Y represents modifier.

System	CA144 (gm)	CH141 (gm)	Modifier (gm)	CR144 (gm)
EP_Control	134.5	121.1	–	2.5
EP_0.05CNT	92	83	4.38	2.5
EP_0.075CNT	86	83	6.56	2.5
EP_0.1 CNT	84	82.8	8.75	2.5
EP_10SiO <sub>2</sub>	57.5	78	45	2.5
EP_20SiO <sub>2</sub>	18.2	62.6	75	2.5
EP_5CSR	72	80	24	2.5
EP_10CSR	54	77	49	2.5
EP_5CSR_10SiO <sub>2</sub>	35	73	24 / 43.7	2.5
EP_0.075CNT_10 SiO <sub>2</sub>	50	78	6.56 / 43.7	2.5
EP_0.075 CNT_5 CSR	66	80	6.56 / 24	2.5

Instruments in 3-points bending mode operating at 1 Hz, on specimens. The glass transition temperature,  $T_g$  of the bulk epoxy samples was determined by the peak value of  $\tan \delta$  curve. The temperature range was set from 0 °C to 180 °C with a heating rate of 3 °C/min.

### 3.3. Electrical conductivity

For some applications in anti-static environments, an inherent electrical conductivity of the composite material is required to dissipate the electrical discharge. The volume conductivities of the CNT composites were determined via a 4-point measurement according to DIN EN ISO 3915 (1999) [26]. The sample size was approximately  $4 \times 4 \times 8 \text{ mm}^3$ . In all cases the samples were cut from the middle of dumbbell shaped specimens and the electrical resistances of the composites were measured. In order to reduce contact resistance, silver conductive paste was applied to the two measuring ends of the sample. The electrical conductivity  $\sigma$  [Siemens / meter] was calculated using the following equation:

$$\sigma = \frac{l}{RA} \left[ \frac{S}{m} \right] \quad (1)$$

where R is the electrical resistance of the specimen; l and A were the sample length and cross-section area, respectively.

### 3.4. Tensile properties

Tensile tests were conducted at 23 °C on a universal testing machine (Instron, USA) in a tensile configuration according to standard DIN EN ISO 527-2 [27]. Dog-bone shape (ISO 527-2 type 1B) samples were used for the testing see Fig. 1. The testing speed was chosen to be 2 mm/min with a 10 kN load cell, a precision sensor-arm extensometer was used to determine the specimen strain.

### 3.5. Fracture tests

The plane strain fracture toughness ( $K_{Ic}$ ) of the composites was determined experimentally at 23 °C by using compact tension (CT) samples under tensile loading conditions according to the Norm ISO 13,586 [28] and at strain rate of 0.2 mm/min. The thickness B and the width W of specimens were chosen to be 4 mm and 36 mm, respectively see Fig. 2. The samples were tested in a universal testing machine (Instron, USA). Prior to testing, a notch was machined and then sharpened by tapping a fresh razor blade into the material, so that a sharp crack was initiated with a length  $a_0$  ( $0.45 \cdot W \leq a_0 \leq 0.55 \cdot W$ ). The fracture toughness  $K_{Ic}$  was then calculated by Equation (2), where F is the maximum force observed in the load-displacement curve, and  $a_0$  is the initial crack length for calculating  $\alpha = a_0/W$  and  $f(a_0/W)$  as follows

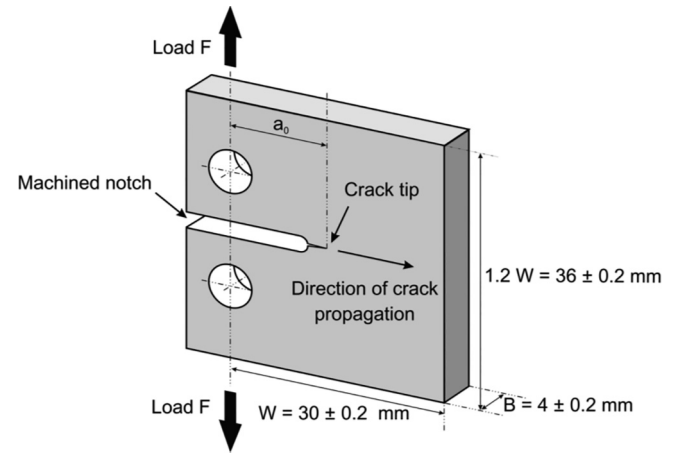


Fig. 2. Compact tension sample geometry used for fracture toughness measurement.

$$K_{Ic} = \frac{F}{B\sqrt{W}} \cdot f(a_0/W) \quad (2)$$

$$f\left(\frac{a_0}{W}\right) = f(\alpha) = \frac{(2 + \alpha)}{(1 - \alpha)^{3/2}} \cdot (0.866 + 4.64\alpha - 13.32\alpha^2 + 14.72\alpha^3 - 5.60\alpha^4) \quad (3)$$

The knowledge of the critical stress intensity factor  $K_{Ic}$ , the elastic modulus  $E_t$  and Poisson's ratio  $\nu$  ( $\sim 0.35$ ) allows calculating the critical energy release rate  $G_{Ic}$ .

$$G_{Ic} = \frac{K_{Ic}^2 (1 - \nu^2)}{E_t} \quad (4)$$

### 3.6. Microscopy studies

The fractured surfaces of the CT tested nanocomposites were studied with the help of a field emission scanning electron microscope (Zeiss Gemini SEM 300). Before scanning, the surfaces of the samples were sputtered with a thin layer of gold for 120 sec using a sputtering device. Transmission electron microscopy (TEM) samples were sectioned using a diamond knife (Diatome, Biel-Bienne, Switzerland) on an ultracut (EM UCT, Leica Microsystems, Vienna, Austria). Ultrathin sections (70 nm) were picked up on copper grids with carbon film. Grids were examined with a Transmission Electron Microscope (Talos F200S G2 - Thermofisher - Eindhoven) at 200 kV, equipped with a 4 K\*4K camera One View (Gatan, Paris (France)).

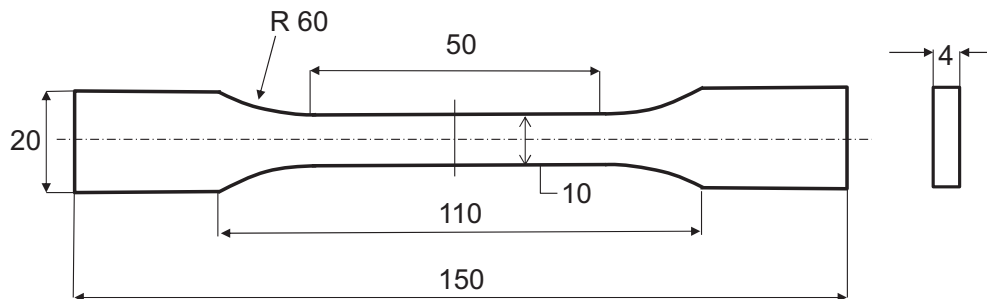


Fig. 1. EN ISO 527-2 type 1B geometry for the tensile test specimen. All dimensions are in mm.

## 4. Results

### 4.1. Electrical conductivity

The electrical conductivity of composites depends on the intrinsic conductivity of polymer and fillers. Polymer have very low electrical conductivities in the range of  $10^{-11}$  to  $10^{-14}$  S/m, however different fillers have higher conductivities. For example, carbon black has conductivity of  $10^5$  S/m, graphite  $10^8$  S/m and pitch based carbon fibers have  $10^6$  S/m [29]. Nanofillers have exceptionally high electrical conductivity and MWCNTs conductivity lies in the range of  $10^4$ – $10^8 \Omega^{-1}\text{m}^{-1}$  [30]. For reference epoxy system and the system with 0.05 wt% of CNT the value to resistance was beyond the measuring limit of the equipment. For 0.075 wt% and 0.1 wt% the conductivity of composite was measured as 0.00026 S/m and 0.00163 S/m respectively (refer Table 2) which shows a trend that with increasing wt% of CNT's in the composites the electrical conductivity will keep on increasing.

### 4.2. Thermal properties

The DSC analysis shows exotherm of reference system as shown in Fig. 3(a). For reference system the peak of exotherm was obtained at  $142^\circ\text{C}$  which further justify the post curing temperature selected for the curing of the formulated systems. The  $T_g$  values of all the systems tabulated in Table 3. The  $T_g$  values of all the systems were calculated using DSC and DMA (DMA) curves however, there was a difference between the  $T_g$  values due to the difference in the principle of measurements and heating rates used.

For reference system the  $T_g$  of  $150^\circ\text{C}$  was reported and with the addition of different nano-fillers  $T_g$  values were reduced for different modified systems as shown in Fig. 3(b). This decrease in glass transition temperature may be due the reason that polymer chains do not have sufficient time to orient themselves in presence of different nano-fillers in prescribed curing schedule and does not form a dense network. This may be the possible reason for the decrease of glass transition of all modified systems. However, researchers reported minor decrease in  $T_g$  values when same type of modifiers were used but longer cure cycles were chosen for the curing process [8,20].

### 4.3. Tensile and fracture properties

The tensile properties of the reference and all modified systems are shown in Table 4. A modulus of 2750 MPa and a tensile strength of 86 MPa were measured for the EP system. The addition of MWCNT's reduces the tensile strength of the epoxies, which was

**Table 3**

Glass transition temperature ( $T_g$ ) of reference and different modified epoxy systems.

System	$T_g$ (DSC) ( $^\circ\text{C}$ )	$T_g$ (tan $\delta$ ) ( $^\circ\text{C}$ )
EP_Control	142	150
EP_0.05CNT	140	145
EP_0.075CNT	130	145
EP_0.1 CNT	126	142
EP_10SiO <sub>2</sub>	126	138
EP_20SiO <sub>2</sub>	125	135
EP_5CSR	138	147
EP_10CSR	135	145
EP_5CSR_10SiO <sub>2</sub>	136	140
EP_0.075CNT_10 SiO <sub>2</sub>	136	145
EP_0.075 CNT_5 CSR	135	140

expected due to possibility of agglomeration while elastic modulus remains the same due to the lower wt% of CNT's used.

For EP\_20SiO<sub>2</sub> system, the tensile strength and tensile modulus were measured as 91 MPa and 3285 MPa respectively which reveals the uniform dispersion and effective adhesion between the epoxy matrix and SiO<sub>2</sub> nanoparticles (see Fig. 4b). The addition of the CSR particles reduced the modulus linearly with increasing content and for EP\_10CSR the tensile strength and tensile modulus were measured as 57 MPa and 2100 MPa respectively, which may be due to the soft core of the CSR particles. For hybrids, the three different systems were prepared with a concentration of CNT, SiO<sub>2</sub> and CSR fixed at 0.075 wt%, 10 wt% and 5 wt% respectively.

The fracture toughness  $K_{Ic}$  and fracture energy  $G_{Ic}$  of the unmodified epoxy and epoxies modified with different nanofillers were measured in mode I using compact tension (CT) tests. The results were summarized in Table 4. The mean values for  $K_{Ic}$  and  $G_{Ic}$  of the unmodified epoxy were determined to be  $0.57 \text{ MPa}\cdot\text{m}^{1/2}$  and  $0.10 \text{ kJ/m}^2$ , respectively. For MWCNT's modified epoxy systems maximum value of  $K_{Ic}$  ( $0.78 \text{ MPa}\cdot\text{m}^{1/2}$ ) and  $G_{Ic}$  ( $0.19 \text{ kJ/m}^2$ ) was achieved at 0.1 wt% of MWCNT. The maximum values of  $K_{Ic} = 1.65 \text{ MPa}\cdot\text{m}^{1/2}$  and the  $G_{Ic} = 1.14 \text{ kJ/m}^2$  were measured for the EP\_5CSR system revealing an increase by a factor of  $\sim 3$  and 11.4 above the unmodified epoxy system. For SiO<sub>2</sub> modified systems maximum values of  $K_{Ic}$  ( $1.55 \text{ MPa}\cdot\text{m}^{1/2}$ ) and  $G_{Ic}$  ( $0.64 \text{ kJ/m}^2$ ) was achieved at 20 wt%. Among hybrid systems maximum value of  $K_{Ic} = 1.75 \text{ MPa}\cdot\text{m}^{1/2}$  and the  $G_{Ic} = 1.01 \text{ kJ/m}^2$  were measured for the EP\_5CSR\_10 SiO<sub>2</sub> system.

### 4.4. Fractographic studies

The toughening mechanisms responsible for the increase in fracture toughness due to the incorporation of different nanofillers can be explained by analyzing the fracture surfaces of the

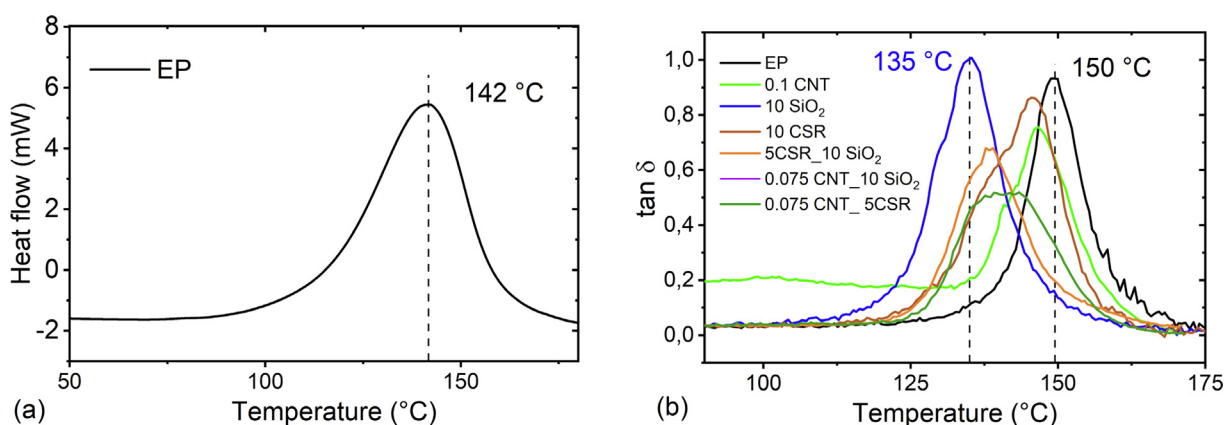


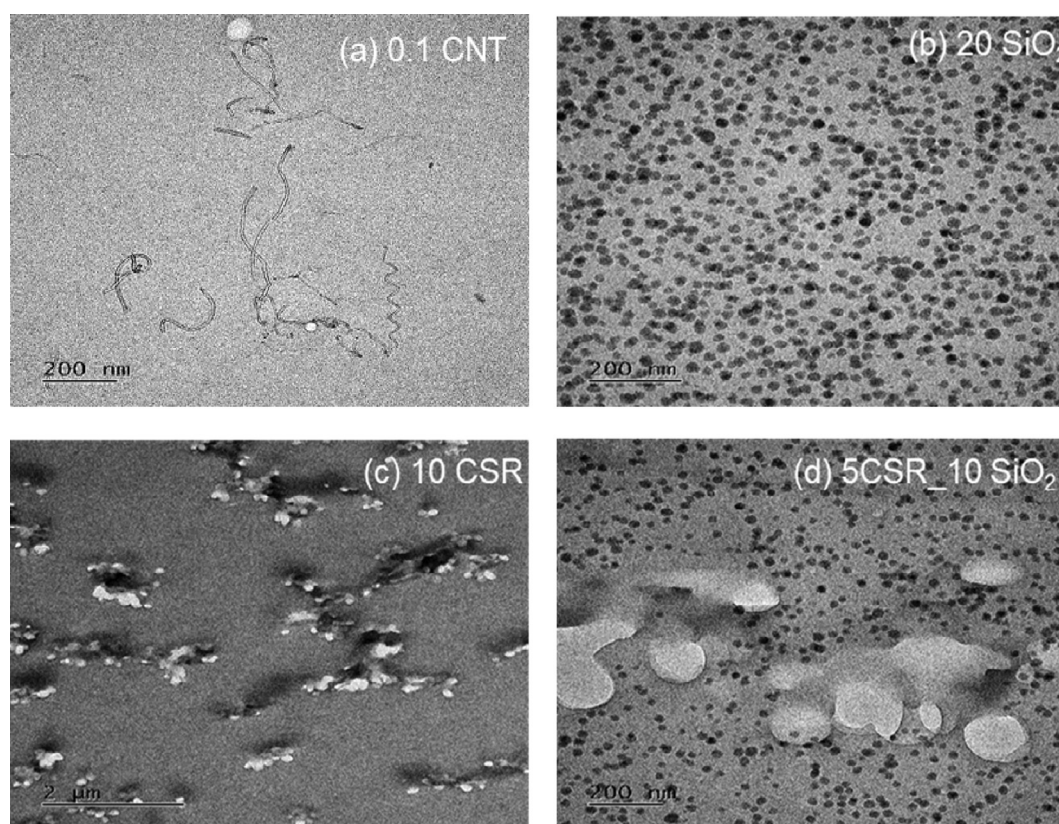
**Fig. 3.** (a) DSC exotherm of reference system and (b) DMA (tan  $\delta$  peak) curve to obtain glass transition temperature of reference and different modified epoxy system.



**Table 4**

Tensile and fracture mechanics properties of reference and modified epoxy systems.

Systems	$E_t$ [MPa]	$\sigma_m$ [MPa]	$\epsilon_m$ [%]	$K_{Ic}$ [MPa·m <sup>1/2</sup> ]	$G_{Ic}$ [kJ/m <sup>2</sup> ]
EP	2750 (±15)	86 (±0.5)	6.6 (±0.1)	0.57(±0.08)	0.10(±0.07)
EP_0.05CNT	2710 (±27)	72 (±0.4)	5.4(±0.2)	0.69(±0.05)	0.15(±0.07)
EP_0.075CNT	2790 (±35)	69 (±0.6)	5.3(±0.2)	0.75(±0.12)	0.18(±0.06)
EP_0.1CNT	2760 (±45)	68 (±0.7)	5.3(±0.1)	0.78(±0.07)	0.19(±0.05)
EP_10SiO <sub>2</sub>	3100 (±17)	89 (±0.9)	6.5(±0.2)	1.30(±0.08)	0.48(±0.06)
EP_20SiO <sub>2</sub>	3285 (±10)	91 (±0.4)	6.8(±0.3)	1.55(±0.10)	0.64(±0.07)
EP_5CSR	2450 (±12)	72 (±0.6)	6.2(±0.4)	1.45(±0.05)	0.75(±0.03)
EP_10CSR	2100 (±24)	57 (±0.6)	5.8(±0.2)	1.65(±0.07)	1.14(±0.04)
EP_5CSR_10SiO <sub>2</sub>	2650 (±17)	71 (±0.8)	5.8(±0.3)	1.75(±0.08)	1.01(±0.06)
EP_0.075CNT_10SiO <sub>2</sub>	2564 (±27)	84 (±0.6)	6.6(±0.2)	1.45(±0.04)	0.72(±0.05)
EP_0.075CNT_5CSR	2470 (±25)	65 (±0.6)	5.4(±0.3)	1.30(±0.06)	0.66(±0.04)

**Fig. 4.** TEM images showing the dispersion of different fillers in modified epoxy systems. (a) EP\_0.1CNT; (b) EP\_20SiO<sub>2</sub>; (c) EP\_10CSR; (d) EP\_5CSR\_10SiO<sub>2</sub>.

unmodified and modified epoxy composites using a field emission scanning electron microscope (FE-SEM). The dispersion of the different nanoparticles used in this work can be observed through transition electron microscopy (TEM). Fig. 4 shows different systems, excellent dispersion was observed for SiO<sub>2</sub> and CSR nanoparticles. The fracture surfaces for the unmodified epoxies, as shown in Fig. 5a, for the anhydride-cured epoxy, show a smooth fracture for inherent brittle epoxy system, which indicate the brittle behaviour of epoxy system during the fracture process.

For CNT modified nanocomposites a uniform dispersion was observed till 0.075 wt%. At 0.1 wt% traces of CNT agglomerates were found at the fracture surface. Debonded CNT's were observed on the fracture surfaces as shown in Fig. 5b. Accordingly, fiber pull-out and debonding was believed to be the dominating toughening mechanisms associated with these CNT's in epoxy. Since van der Waals forces create a mutual attraction of the CNT's they can push CNT cluster into agglomerates in the epoxy matrix even after

proper dispersion processes [31]. The presence of agglomerates was known to reduce the material's toughness and ability to resist fracture [8]. This might be a reason, why the addition of the CNT has only little effect on the toughening of epoxy. Though the higher concentration of CNT's increases the stiffness of the material but at the same time stress concentration caused by the CNT agglomerates initiated the crack and lead to fracture of the nanocomposites see Fig. 5e.

The fractographic analysis of the fracture surface of SiO<sub>2</sub> modified epoxy resin with the help of SEM and TEM can give an insight into the cause and location of failure, as well as the dispersion state of the particles within the epoxy matrix respectively. Fig. 5d shows a close up of the crack surface in a nanocomposite containing 5CSR\_10SiO<sub>2</sub> nanoparticles, some nano and micro reinforcing mechanisms can be observed with more detail. Some of these mechanisms include shear yielding, crack deflection, and particle crack pinning as indicated by the small tails behind the particles.

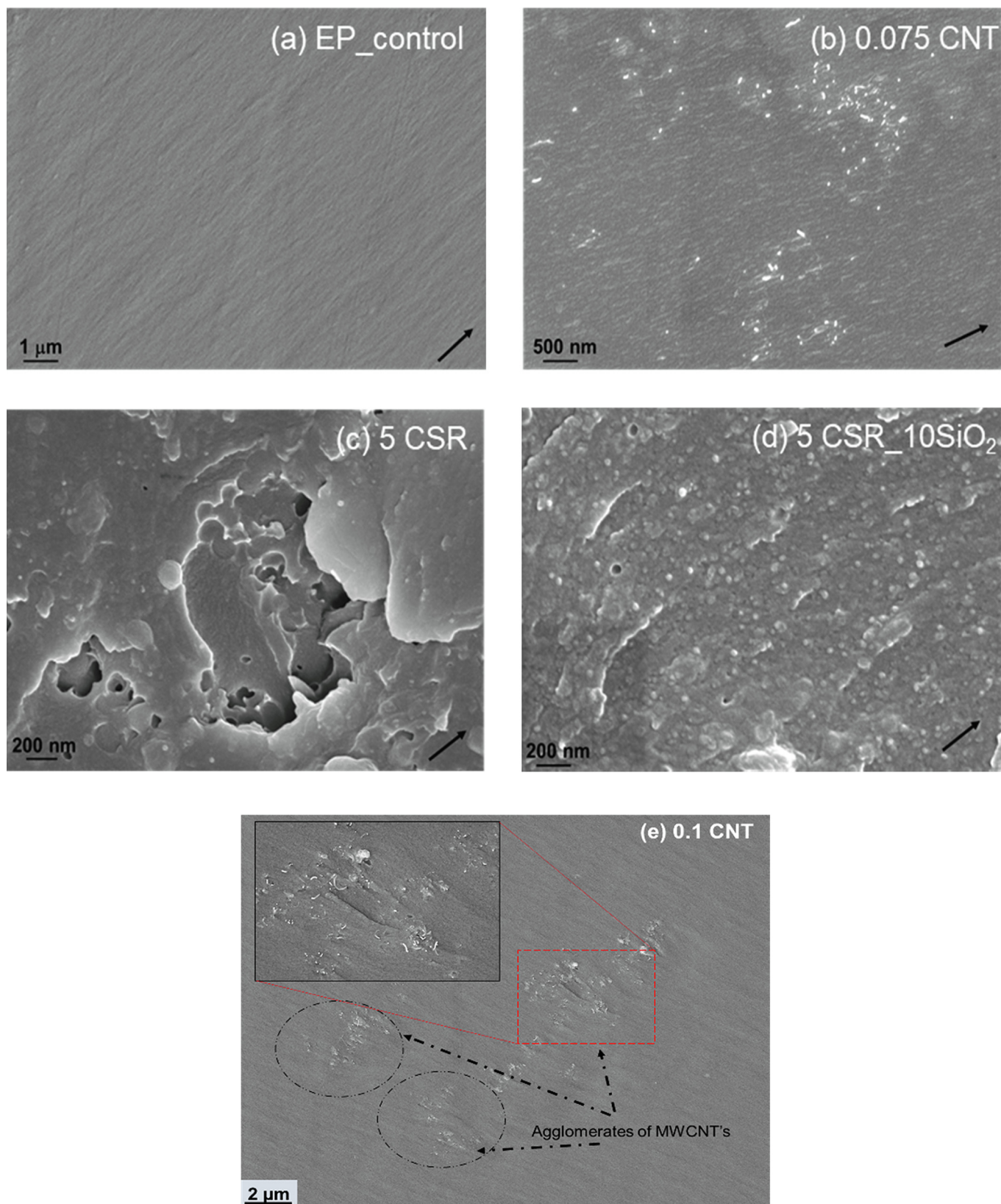


**Fig. 5.** FEG-SEM micrographs of the fracture surface of the different modified systems. Black arrow showing the direction of crack propagation. (a) EP; (b) EP\_0.075CNT; (c) EP\_5CSR; (d) EP\_5CSR\_10SiO<sub>2</sub>; (e) 0.1 CNT.



Similarly for CSR modified systems river lines and ridges were observed on CSR modified systems along with voids which formed due to the cavitation of core of the CSR nanoparticles see Fig. 5c.

## 5. Conclusion

The material properties of an anhydride hardener cured bisphenol A based epoxy modified with CNT's, rigid pre-dispersed SiO<sub>2</sub> nano-particles, CSR nanoparticles and hybrid of SiO<sub>2</sub>\_CNT and CSR\_CNT were investigated in terms of tensile, fracture mechanics properties, electrical properties and thermo-mechanical properties, which further correlated with microstructural features and toughening mechanisms. For CNT's based epoxy nanocomposites the electrical conductivity was threshold value was obtained for 0.075 wt%. Further hybridisation with CSR and SiO<sub>2</sub> maintain the value of electrical conductivity with simultaneous improving the tensile and fracture properties.

## CRedit authorship contribution statement

**A. Bajpai:** Conceptualization, Methodology, Writing - original draft, Investigation. **R. Martin:** Formal analysis, Project administration, Funding acquisition. **H. Faria:** Formal analysis. **E. Ibarboure:** Formal analysis. **S. Carlotti:** Supervision, Funding acquisition.

## Declaration of Competing Interest

The authors declare that they have no known competing financial interests or personal relationships that could have appeared to influence the work reported in this paper.

## Acknowledgements

"This work was financed by ERDF funds through the V Sudoe Interreg program within the framework of the COMPRESSer project, Ref. SOE2/P1/E0643". Imaging was performed on the Bordeaux Imaging Center, member of the France Bio-Imaging national infrastructure (ANR-10-INBS-04). We thank S. Lacomme for her TEM work on this project.

## References

- [1] U.P. Breuer, *Commercial Aircraft Composite Technology*, Springer International Publishing, 2016.
- [2] A. Bajpai, B. Wetzel, K. Friedrich, High strength epoxy system modified with soft block copolymer and stiff core-shell rubber nanoparticles, *Express Polymer Lett.* 14 (4) (2020) 384–399.
- [3] R.A. Pearson, A.F. Yee, Toughening mechanisms in thermoplastic modified epoxies. 1. Modification using poly(phenylene oxide), *Polymer* 34 (1993) 3658–3670.
- [4] R.A. Pearson, A.F. Yee, Toughening mechanisms in elastomer-modified epoxies, *J. Mater. Sci.* 24 (7) (July 1989) 2571–2580.
- [5] A.F. Yee, R.A. Pearson, Toughening mechanisms in elastomer-modified epoxies Part 1 Mechanical studies, *J. Mater. Sci.* 21 (1986) 2462–2474.
- [6] K.F. Lin, Y.D. Shieh, Core-shell particles designed for toughening the epoxy resins. II. Core-shell-particle-toughened epoxy resins, *J. Appl. Polym. Sci.* 70 (12) (1998) 2313–2322.
- [7] A. Klingler, A. Bajpai, B. Wetzel, The effect of block copolymer and core-shell rubber hybrid toughening on morphology and fracture of epoxy-based fibre reinforced composites, *Eng. Fract. Mech.* 203 (2018) 81–101.
- [8] A. Bajpai, A.K. Alapati, B. Wetzel, Toughening and mechanical properties of epoxy modified with block co-polymers and MWCNTs, *Procedia Struct. Integrity* 2 (2016) 104–111.
- [9] A. Bajpai, A. Alapati, A. Klingler, B. Wetzel, Tensile properties, fracture mechanics properties and toughening mechanisms of epoxy systems modified with soft block copolymers, rigid TiO<sub>2</sub> Nanoparticles And Their Hybrids, *J. Compos. Sci.* 2 (4) (2018) 72.
- [10] B. Wetzel, P. Rosso, F. Hauptert, K. Friedrich, Epoxy nanocomposites – fracture and toughening mechanisms, *Eng. Fract. Mech.* 73 (2006) 2375–2398.
- [11] J. Lee, A.F. Yee, Fracture of glass bead/epoxy composites: on micro-mechanical deformations, *Polymer* (2000).
- [12] T.H. Hsieh, A.J. Kinloch, K. Masania, A.C. Taylor, S. Sprenger, The mechanisms and mechanics of the toughening of epoxy polymers modified with silica nanoparticles, *Polymer* 51 (26) (2010) 6284–6294.
- [13] Y.L. Liang, R.A. Pearson, The toughening mechanism in hybrid epoxy-silica-rubber nanocomposites, *Polymer* 51 (2010) 4880–4890.
- [14] T.H. Hsieh, A.J. Kinloch, K. Masania, J. Sohn Lee, A.C. Taylor, S. Sprenger, The toughness of epoxy polymers and fibre composites modified with rubber microparticles and silica nanoparticles, *J. Mater. Sci.* 46 (11) (2011) 4092.
- [15] D. Maxwell, R.J. Young, A.J. Kinloch, Hybrid particulate-filled epoxy-polymers, *J. Mater. Sci. Lett.* 3 (1) (1984) 9–12.
- [16] D. Carolan, A. Ivankovic, A.J. Kinloch, S. Sprenger, A.C. Taylor, Toughening of epoxy-based hybrid nanocomposites, *Polymer* 97 (2016) 179–190.
- [17] A. Bajpai, S. Carlotti, The effect of hybridized carbon nanotubes, silica nanoparticles, and core-shell rubber on tensile, fracture mechanics and electrical properties of epoxy nanocomposites, *Nanomaterials* 9 (7) (2019) 1057.
- [18] Y.T. Wang, C.S. Wang, H.Y. Yin, L.L. Wang, H.F. Xie, R.S. Cheng, Carboxyl-terminated butadiene-acrylonitrile-toughened epoxy/carboxyl-modified carbon nanotube nanocomposites, *Express Polym. Lett.* 6 (9) (2012) 719–728.
- [19] G. Szebenyi, L. Tóth, J. Karger-Kocsis, Effect of an ionic liquid on the flexural and fracture mechanical properties of EP/MWCNT, *MSF (Materials Science Forum)* 885 (2017) 19–24.
- [20] A. Bajpai, B. Wetzel, A. Klingler, K. Friedrich, Mechanical properties and fracture behavior of high-performance epoxy nanocomposites modified with block polymer and core-shell rubber particles, *J. Appl. Polym. Sci.* 136 (46) (2019) 48471.
- [21] C.B. Duke, Metal-filled polymers—properties and applications, *J. Polym. Sci. C Polym. Lett.* 25 (6) (1987) 263.
- [22] Y.P. Mamunya, Y.V. Muzychenko, P. Pissis, E.V. Lebedev, M.I. Shut, Percolation phenomena in polymers containing dispersed iron, *Polym. Eng. Sci.* 42 (1) (2002) 90–100.
- [23] Y.X. Zhou, P.X. Wu, Z.-Y. Cheng, J. Ingram, S. Jeelani, Improvement in electrical, thermal and mechanical properties of epoxy by filling carbon nanotube, *Express Polym. Lett.* 2 (1) (2008) 40–48.
- [24] "Product Data Sheet Biresin CR144," 2017.
- [25] N.V. Kaneka Belgium, Technical Data Sheet- Kane Ace Trade Mark, Brussels, Belgium, 2015.
- [26] DIN EN ISO 3915 : 1999 Plastics - Measurement of resistivity of conductivity plastics, German Institute for Standardisation, 1999.
- [27] ISO 527-2: Tensile Testing for Plastics, International Organization for Standardization, 2012.
- [28] ISO 13586:2000(E): Plastics – Determination of fracture toughness (GIC and KIC) – Linear elastic fracture mechanics (LEFM) approach, Switzerland: ISO (the International Organization for Standardization).
- [29] A. Demain, J.P. Issi, The effect of fiber concentration on the thermal conductivity of a polycarbonate/pitch-based, *J. Compos. Mater.* 27 (7) (1993) 668–683.
- [30] N. Grossiord, J. Loos, L.C. Laake, M. Maugey, C. Zakri, C.E. Koning, A.J. Hart, High conductivity polymer nanocomposites obtained by tailoring the characteristics of carbon nanotube fillers, *Adv. Funct. Mater.* 20 (18) (2008) 3226–3234.
- [31] P. Ma, S. Mo, B. Tang, J. Kim, Dispersion, interfacial interaction and re-agglomeration of functionalized carbon nanotubes in epoxy composites, *Carbon* 48 (6) (2010) 1824–1834.